



Morphotectonics of Mount Rendingan Area Related To the Appearances of Geothermal Surface Manifestations

DEWI GENTANA^{1,2}, NANA SULAKSANA², EMI SUKIYAH², and EUIS TINTIN YUNINGSIH²

¹Postgraduate Program of Geology, Faculty of Geological Engineering, Padjadjaran University,
Jln. Raya Bandung - Sumedang Km. 21, Jatinangor, Sumedang, Indonesia

²Faculty of Geological Engineering, Padjadjaran University,
Jln. Raya Bandung - Sumedang Km. 21, Jatinangor, Sumedang, Indonesia

Corresponding author: dewigentana06@gmail.com

Manuscript received: May, 23, 2018; revised: January, 15, 2019;

approved: May, 20, 2019; available online: December, 9, 2019

Abstract - The researched area is situated at Mount Rendingan and its surrounding area, Lampung Province, the southern part of Sumatra Island. It has a big potential of geothermal resource in line with a unique graben like bowl landform and geothermal surface manifestations. This research was carried out using remote sensing and field observation methods. The remote sensing method used topography and Shuttle Radar Topography Mission -Digital Elevation Model (SRTM-DEM) maps to analyze morphotectonic attributes, and the result was validated by morphotectonic data analysis from field observation. The purpose of this research is to evaluate the relation between morphotectonic and the appearances of geothermal surface manifestations. The interpretation of SRTM-DEM and topographic maps are supported by morphotectonic analyses, which indicate that the geothermal surface manifestations in this area are controlled by tectonic activity. It has various levels of lift which are shown by the values of valley height weight ratio (V_r) from 0.16 to 3.31 and the values of mountain front sinuosity (S_{mf}) from 1.05 to 2.09. The morphotectonic characteristics can describe the geological structure activity levels which are reflected in the landform and its rock. The volcanic areas consist of igneous rocks which have small primary permeabilities. However, the development of geological structure can cause fractures in the rock that step in as a medium for passing geothermal fluid from depth to surface. They are found on the fault intersection zone system trending NE-SW and NW-SE, NNE-SSW and NNW-SSE, and WE system directions that indicate the fault system is correlated with the appearances of geothermal manifestations.

Keywords: morphotectonics, geothermal surface manifestation, SRTM-DEM Image, V_r , S_{mf}

© IJOG - 2019. All right reserved

How to cite this article:

Gentana, D., Sulaksana, N., Sukiyah, E., and Yuningsih, E.T., 2019. Morphotectonics of Mount Rendingan Area Related To the Appearances of Geothermal Surface Manifestations. *Indonesian Journal on Geoscience*, 6 (3), p.291-309. DOI: [10.17014/ijog.6.3.291-309](https://doi.org/10.17014/ijog.6.3.291-309)

INTRODUCTION

Indonesia is geologically positioned in a convergent zone between Indian Oceanic Plate and Eurasian Continental Plate. This convergent zone is seismically active with many active volcanoes. The 62 % global distribution of volcanoes in the world is concentrated around the margin

of Pacific Ocean which is called Ring of Fire. About 14% of the volcanoes are located in the Indonesian island arcs which are part of Alpine-Indonesian volcano mountain belt (Kirianov, 2007). The researched area, Mount Rendingan and its surrounding area, is situated in Tanggamus District of Lampung Province, southern part of Sumatra, Indonesia that has geothermal

potential. Based on its physiography, this area is a part of the Southern Semangko Zone which has a depression area along Bukit Barisan with NW to SE direction trend. McCaffrey (2009) stated that the Semangko Fault was an active fault in the mainland that divided the Sumatra Island, extending along the Bukit Barisan Mountains from Semangko Bay to Banda Aceh. Muljana (2006) stated that changes in speed and direction of subduction between Indo-Australian Plate to Eurasia Plate were the response to the formation of normal faults with graben pattern in the Sunda Strait where the researched area was situated.

The regional tectonic is characterized by a depression formed along the convergent boundary in subduction zones where the volcano is located. It is commonly accompanied by numerous lo-

cal faults (Zobin, 2017). The subduction zone of Sumatra is an Indo-Australian Plate under the Eurasian Plate, whereas the Indo-Australian Plate moves northward with a relative velocity to the Eurasian Plate of 7 cm/year (Wilson *et al.*, 1998 in Handayani *et al.*, 1998). Tectonic activities lead to deformation and trigger the formation of fractures (Keller, 1986). In addition, tectonic also causes the occurrence of geohazard such as earthquake, landslide, and tsunami (O'Rourke *et al.*, 2016). The researched area has a very complex geological structure relating to the tectonic development of Sumatra Island. It lies in the intra-arc volcanic zone within the Sumatra Island tectonic system. According to McCaffrey (2009), this area is part of volcanic arc zone which is controlled by Sumatra subduction zone (Figure 1).

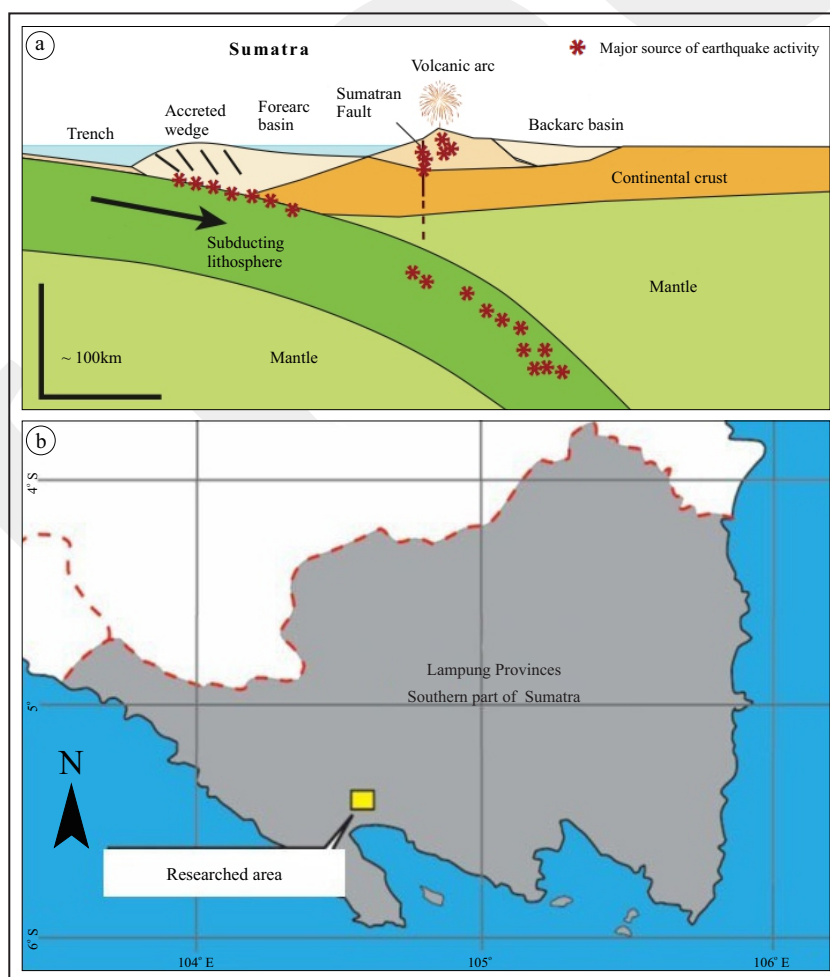


Figure 1. Geological cross-section of volcanic arc zone related to the position of research area that associates with the development of Sumatra Island tectonics (McCaffrey, 2009), where (a) the cross-sectional line corresponding to the existence of Sumatra Fault, (b) the research area located in the southern part of Sumatra Island.

Bhatet *al.* (2013) stated that ridge, plateau, hill, alluvial fan, canyon, terrace, slope, dune, river etc.were collection of an area called landscape. The development of landscape form is strongly influenced by the occurrence of geological structures on the earth. Therefore, the landscape assessment could identify the geological processes occurring in the researched area. Landform assessment can be done with qualitative and quantitative (morphotectonic) points of view. The results of these assessments reflect the degree of tectonic activity occurring in the past, because morphology has the dimension of space and time. Doornkamp (1986) stated that the morphological form was related to tectonic activity characterized by the presence of shutter ridges, fault escarpments, and lakes.

The characteristics of the landscape are enriched through morphotectonic understanding of the ridge, valley lineament, cliff, hill form, and lineament of rivers or certain river patterns. Keller (1986, in Bhat *et al.*, 2013) stated that information about the tectonic history of an area could be retrieved by quantification of different morphotectonic indices after obtaining important information from topographic maps, aerial photographs, and satellite data. Morphotectonic analysis is an approach to determine the level of activity of a fault through observation of the direction of lineaments of ridge, hill, valley, and river segments. Morphotectonic characteristic can describe the degree of active geological structure reflected by the landform and its rock.

Fault is a fracture or cracking system within rocks that has undergone movement. A collection of interconnected faults is called a fault zone. The definition of an active fault is a fault that has been in motion ten million years ago, and a potential active fault is a fault that had moved about two million years ago or during Quaternary and potentially reactivated. The inactive fault is a fault that has not moved in the past two million years (Keller and Printer, 1996).

Regionally, the tectonic activity developing in the researched area originates from a chain of tectonic activity that takes place along the

Sumatra Island bundle, forming a continuous Semangko Fault from the south to the north, or vice versa. The pattern of this structure causes the cutting of the rocks creating a weak area. The structure of the landscape in the form of a steep escarpment, usually form a weak zone as a medium of geothermal fluid flowing to the surface. According to Siahaan (1988) the depression of the researched area is dominated by two principal directions of lineament: the antithetic NW - SE and NNW - SSE lineaments of the Semangko Fault system existing as secondary faults and the NE - SW direction which is part of Semangko System. Gentana *et al.* (2017) studied the lineament interpretation using topographic contour map, emphasizing the lineament features by calculating every single triangle that used micromine software with the result azimuth of N 270° E - N 310° E. The lineament shows NW - SE, NE - SW, NE - SW, and WE directions with 30° - 65° slope variations. In the researched area, NE - SW lineaments are dominant that control the appearances of geothermal surface manifestations. While Sukiyah *et al.* (2015) described that morphotectonic analysis showing the landform could be identified by using satellite imagery. Furthermore, based on the image analysis of Digital Elevation Model-Shuttle Radar Topography Mission (SRTM-DEM), the main pattern of the structures in the researched area is fault occurring as the second order of the Semangko Fault (Figure 2).

According to McCaffrey (2009), Sumatra Fault along the Bukit Barisan causes active volcanoes, whereas the studied area is formed by tectonic and volcanic phenomena which create a depressed area. The development of tectonic activities created from chain regional phenomenon forming Sumatra Island led to the presence of Semangko Fault zone expanded from the south to the north. This area is characterized by complex structural and lithological conditions. Moreover, the structural and lithological analyses were used to identify the availability of two elements such as the combination of fractures with rocks of one another. The contact of rock sometimes occurs as

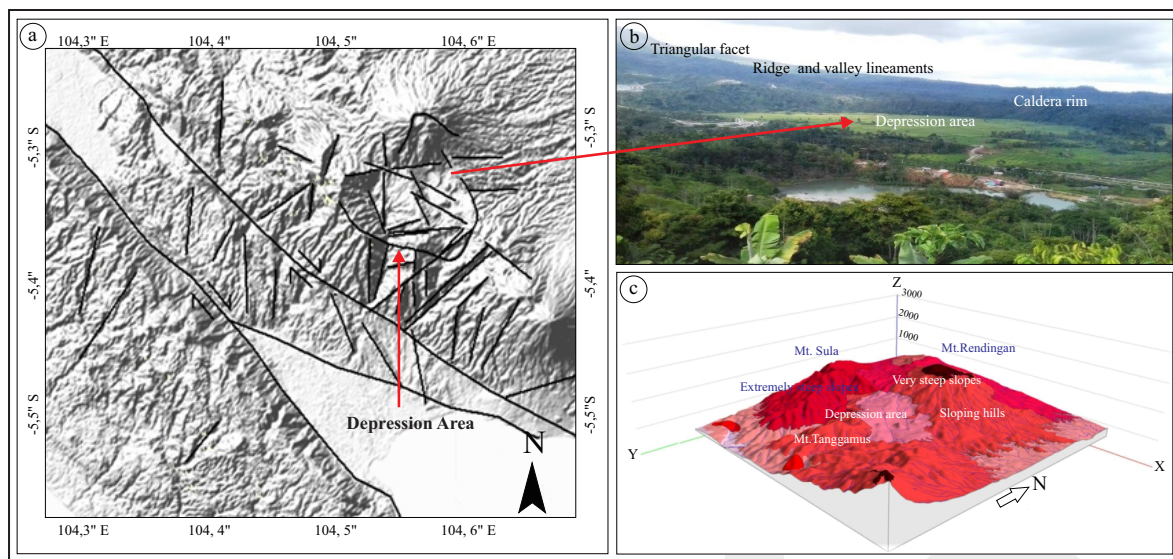


Figure 2. a). Semangko strike-slip dip dextral fault system (based on DEM-SRTM image), (b) Morphology of steep hill and valley, triangular facet, and depression area (based on field observation), and (c) 3 D model of morphology in the research area showing extremely steep mountain slope until plain (depression) area.

a slicken-side of the fault commonly normal fault (gravity fault). Microseismic distribution was used as tools for searching a permeable rock zone. The level of seismicity can control the appearance of the surficial geothermal manifestations, where the greater the level of seismicity, the greater the debit of geothermal fluid flow (Kamah, 2001).

METHOD

The objective of the research is to reveal the morphological and geological structures of the landform ridge lineament, valley, mountain or hill, river curve, and fault based on SRTM-DEM image and a topographic map. The research method carried out can be divided into two types. They are remote sensing and field observation methods. The first method was carried out by interpreting the topographic maps, SRTM-DEM image, and morphotectonic analysis. The effect of tectonic activity and landform can be observed by a digital topography map with a high resolution imagery (Scheidegger, 2004).

The field method includes observation of geological structure and geothermal surface manifestation distribution in the field. According to Hancock (1994), part of the geomorphological

study that learns the relationship among geological structures is called morphotectonic. The morphotectonic characteristic of each watershed was examined through the calculations of valley floor width to valley height ratio (V_f) and sinuosity mountain front (S_{mf}). Topography and geological characters influence the watershed function (Van Noordwijk *et al.*, 2004). Furthermore, Linsley *et al.* (1949) stated that the drainage area of interconnected river system downstream into a single outlet was called watershed.

The morphometric analysis of drainage networks was devised to be used explicitly in tectonic environments, such as the ratio of valley floor width to valley height (Bull and McFadden, 1977). The morphotectonic analysis was done by processing all the data, especially related to the topography map data and satellite imageries by observing the landform. Morphotectonic variables can be used to measure tectonic activity level reflected by the shape and dimensions of the slope, valley, and ridge. The result of morphotectonic analysis is used to determine a relationship between morphotectonic characteristic and the distribution of geothermal manifestations at the surface.

The landform conditions and the level of tectonic activity are reflected by the geomorphic

index, *i.e.* valley floor width to the valley height ratio (V_f) and sinuosity mountain front (S_{mf}) described as below:

Valley Floor Width to Valley Height Ratio (V_f)

The ratio of the width and height of the valley is a value of the valley area that characterizes the uplift of an area. High V_f values reflect low uplift rates and have a tilted or lateral shape of the valley having the shape of the “U” basin, whereas for areas with high elevation rates the valleys tend to be narrower or “V” (Keller and Pinter, 1996). Goudie (2004) stated that high values of V_f area associated with low uplift rates had enabled streams to cut broad valley floors. While low values of V_f area associated with high uplift rate. The use of such combination indices particularly, enables the production of relative tectonic activity class designation for area. The V_f value is calculated using the equation:

$$V_f = \frac{2Vfw}{(Eld - Esc) + (Erd + Esc)} \dots\dots\dots (1)$$

Where:

- V_f : Valley floor width to height ratio
- Vfw : Wide of the valley floor
- $Eld - End$: Elevation of the left and right of the valley respectively
- Esc : Elevation of the valley floor

Sinuosity Mountain Front (S_{mf})

Sinuosity mountain front (S_{mf}) is an index that reflects a balance between tectonic forces and the strength of erosion. The active tectonic force tends to form a relatively straight face of the mountain with has a low S_{mf} value. While the face of an inactive mountain will form an irregular mountain face (squiggly), due to the role of erosion (Doornkamp, 1986). Bull and McFadden, 1977; in Doornkamp, 1986), stated that the mountain front sinuosity (S_{mf}) was a comparison between the length of the front of the mountain (L_{mf}) and the length of the mountain front projection into the plane area (L_s). Goudie (2004) stated that sinuosity mountain front was an index reflecting the balance between erosional forces that tend

to cut embayment into a mountain front and the tectonic forces that tended to produce a straight front coincident with an activity range-boundary fault. In addition, Yudhicara *et al.* (2017) stated that the intensive uplift was indicated by a low S_{mf} value. Given mountain fronts which associate with active tectonics are straight; they have low values of S_{mf} . The S_{mf} value is calculated using the equation:

$$S_{mf} = \frac{L_{mf}}{L_s} \dots\dots\dots (2)$$

Where:

- S_{mf} : Mountain front sinuosity
- L_{mf} : The length at pronounced break in slope (km)
- L_s : The straight line length of the mountain front (km²)

Lineament density (L_d)

Lineament Density (L_d) is a method used to assess highly structure density areas formed by the interconnection of faults and fractures or lineaments. This method utilizes digital topography data to delineate the lineaments morphology which appears as the response to active tectonics. Soengkono (1999), the line intensity can be counted by simple mathematical equation derived from the total length of straightness in each one unit area and used in localizing zones with high fracture intensity which is calculated by the equation:

$$L_d = F/A \dots\dots\dots (3)$$

Where:

- F: is lineament frequency
- A : is area of calculation (km²)

The density of these lineaments over the study area are shown by the density of this lineament in every section of the grid of 1 km x 1 km. The density defines as the total length of the lineaments within each grid block. Thus, the unit for the density is km⁻¹. This method is used in volcanic terrain of geothermal fields where

fracture zones that have high lineament density indicate the permeable zone associated with geothermal fluid at depth.

The field method is done by observing directly the landscape phenomenon related to the geological structure. Studio analysis and field observation were conducted to ensure that the interpretation of the studio data was inline with the actual conditions in the field.

The data used for morphological interpretation are SRTM-DEM image and topographic map of 1:25,000 scaled. Interpretation on satellite imagery was viewed by visually observing the colours, tones, shapes, patterns, and textures. The SRTM-DEM data and the other data were used to confirm all data validation related to the geothermal surface manifestation distributions in the field.

The research methods include geomorphology, tectonic activity level, ridge, valley lineament, and morphotectonic as well as geological structure analysis. They were supported by field observation illustrated in the following flowchart shown in Figure 3.

RESULT

This part explains a relationship between the result of remote sensing analysis and field interpretation based on the present valid data related to the tectonic activity which was found in the researched area. Besides, it also explains physical properties and distribution of geothermal surface manifestation related to the role of the existing faults.

Geomorphology

The research was conducted at Mount Rendingan and its surrounding area. By observing the ridge and valley lineaments on topographic maps and SRTM-DEM image, it is expected to know tectonic features such as fault. Linear features, depression zones, contrast elevation in a region are reflections of tectonic responses that are generally form fracture zones which is controlled by geological structures (Wilson, 2000; Burbank and Anderson, 2001; Ritter *et al.*, 2002; Scheidegger, 2004; Ganas *et al.*, 2005; Jelínek., 2008).

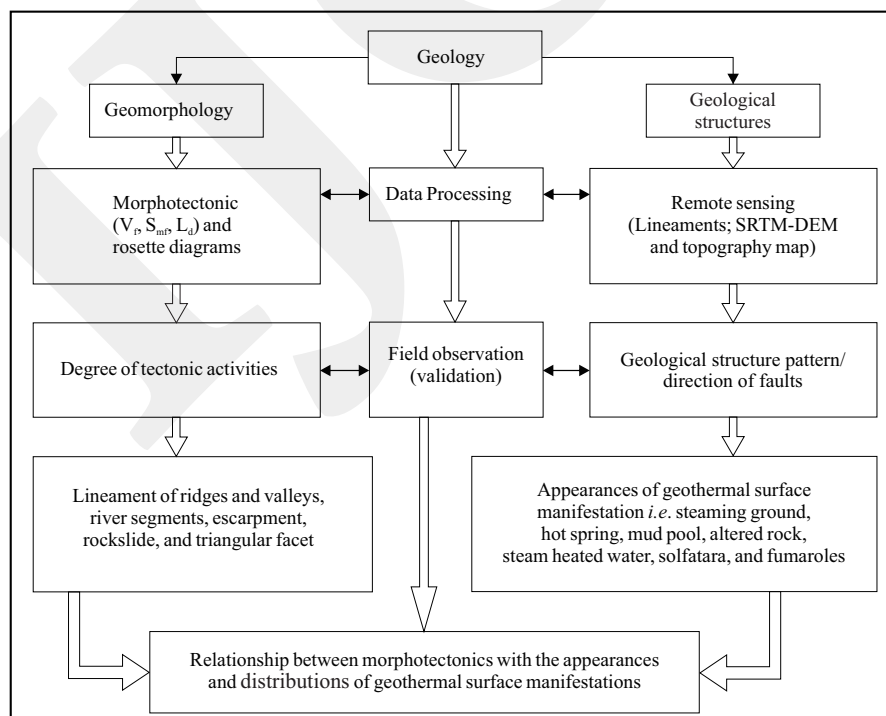


Figure 3. Flow chart of research stage to determine the relationship between morphotectonics with the appearances and distribution of geothermal manifestation in the surface through remote sensing morphology and quantitative analysis (V_t and S_{mp} and L_d) that expresses geological structure, supported by field observation.

The morphology in the researched area can be divided into several units based on the morphological feature such as elevation, slope, lithology, *etc.* Variations in morphological condition are caused by several factors such as lithological diversity and geological endogen/exogen process (Van Zuidam, 1983). The researched area and its surroundings are occupied by steep hills and plain area landforms from the south to the north with the highest elevation are Mount Tanggamus ($\pm 2,156$ m a.s.l.), Mount Rendingan ($\pm 1,608$ m a.s.l.), and Mount Sula ($\pm 1,421$ m a.s.l.), whereas the lowest elevation is Way Panas Village (± 50 m a.s.l.). The morphological units lying on the volcanic area comprise eight morphologies. The highest morphology is about 67% slope and the lowest is about 3% slope (depression area). It consists of volcanic sloping low hills at the elevation of 125 - 200 m a.s.l. with slope class is sloping (8.7 - 12.2%), volcanic steep hills at the elevation of 200 - 500 m a.s.l. with slope class is steep (8.7 - 28.6%), volcanic

plain plateau at the elevation of 700 - 875 m a.s.l. with slope class is almost flat (3.4 - 6.9%). Meanwhile, volcanic sloping high hills were found at the elevation of 500 - 1,275 m a.s.l. with the slope class is sloping (8.7 - 14%), volcanic steep high hills at the elevation of 500 - 1,500 m a.s.l. with slope class is steep (19.4 - 67%), and volcanic very steep high hills found at the elevation of 750 - 1,275 m a.s.l. with slope class is very steep (26.7 - 50.9%). Furthermore, there are volcanic extremely steep mountain at the elevation of 1,500 - 1,975 m a.s.l. with slope class is extremely steep (30.5 - 64.9%), and volcanic steep hills at the elevation of 175 - 625 m a.s.l. with slope class is sloping. The over all of the western part of the researched area consists of steep hills morphology, while the middle part is occupied by plain morphology. This contrast morphological difference is caused by some geological factors such as geological structure process (Van Zuidam, 1983). The morphological unit classification is described in Table 1.

Table 1. Geomorphological Unit in the Research Area is composed of Eight Morphology that has a low Slope Steepness (plains) with have Slope Ranges of 8.7 - 64.9% at Elevation 125 - 625 m above sea level (Van Zuidam, 1983)

Morphology Unit	CS	Morphology Characteristics								
		Morphography			Morphometry			Morphogenetic Process		Lithology
		Drainage Pattern	Valley Shape	Land-form	Elevation (asl)	Slope (%)	Slope Class	Endogen	Exogen	
Volc ^{*1} Sloping Low Hills		Sub-Parallel		U - V Hills 125 - 200		8.7 - 12.2	Sloping	Volc ^{*1}	Erosion	b,l,t ^{*2}
Volc ^{*1} Steep Hills		Sub-Parallel Sub-Dendritic, Sub-Trellis		U - V Hills	200 - 500	8.7 - 28.6	Steep	Volc ^{*1}	Erosion	b,l,t ^{*2}
Volc ^{*1} Plain Plateau		Sub-Parallel	V	Plain	700 - 875	3.4 - 6.9	Almost flat	Volc ^{*1}	Erosion	b,l,t ^{*2}
Volc ^{*1} Sloping High Hills		Sub-Parallel	V	Hills	500 - 1275	8.7 - 14	Sloping	Volc ^{*1}	Erosion	b,l,t ^{*2}
Volc ^{*1} Steep High Hills		Sub-Parallel, Sub-Dendritic, Sub-Trellis	V	Hills	500 - 1500	19.4 - 67.4	Steep - E. ^{*4} steep	Volc ^{*1}	Erosion	b,l,t ^{*2}
Volc ^{*1} Very Steep High Hills		Sub-Annular	V	Hills	750 - 1275	26.7 - 50.9	Very Steep	Volc ^{*1}	Erosion	b,l,t ^{*2}
Volc ^{*1} Extremely Steep Mountain		Sub-Parallel, Sub-Dendritic	V	Mountain	1500 - 1975	30.5 - 64.9	Steep - E. ^{*4} steep	Volc ^{*1}	Erosion	b,l,t ^{*2}
Volc ^{*1} Steep Hills		Sub-Parallel	V	Hills	175 - 625	17.6 - 26.8	Steep	Volc ^{*1}	Erosion	IG ^{*5}

volc^{*1}.= volcanic ; b,l,t^{*2}= breccia, lava, tuff ; CS^{*3}=Colour Symbol; E.^{*4}=Extremely; IG^{*5}=Intrusive Granite

Geological Structure

A detailed structural analysis has been carried out at Mount Rendingan and its surrounding area in order to characterize the tectonic activity level related to the distribution of geothermal surface manifestations. Based on the SRTM-DEM image and topographic map analysis supported by rosette diagram, this area is dominated by two principals of the NW - SE and NE - SW trending faults. The NW - SE lineament of ridges (N 294° - 336°) indicates a structure along the northern and western parts of this area. The NE - SW lineament of valleys (N 24° - 57°) has a trend structure along the southeastern-eastern part of this area.

Other faults displaying NNW - SE, NNE - SSW, NNW, and W - E directions have also been recognized in the northern and eastern parts in the researched area. In addition, the NW - SE trending faults are associated with the direction of the Semangko Fault System. The NNW - SSE fault system is in pairs with NNE to SSW, while the NW to SE fault system forming a pair with NE to SW part of the Semangko Fault System. Active fault is a fault which is moving at a period of ten thousand years ago (Keller and Pinter, 1996). Furthermore, the area of fracture which is followed by a relative movement of the rock block each other is defined as a fault. The displacement of distance and the zone ranges from a few millimetres to ten of kilometres (Sukiyahet *et al.*, 2016). The NNW - SSE fault in this area is evidenced by the rockslide, ridge and valley lineaments, fault scarp, and triangular facet along the western ridge. It indicates that the fault is active.

Morphotectonic

The morphotectonic features of Mount Rendingan and its surrounding area are represented by elongated hills that indicate as geological structures with an altitude 1 - 3 m and about 200 m fault scarp. Four main systems of fault direction can be distinguished: NNW-SSE direction (the average direction N345°), W - E (the average direction N 85°), NE - SW (the average direction N43°), and NW - SE (the average direction N315°). The NW - SE trending structure is similar to the

main regional tectonic (Semangko Fault System), whereas the NNW - SSE, W - E, and NE - SW trending directions are predicted as minor faults of Semangko Fault System.

The morphometric parameter to identify the level of tectonic activity on a region used geomorphic parameters such as valley floor width to height ratio (V_f) and sinuosity mountain front (S_{mf}). Sukiyah *et al.* (2015) stated morphotectonic characteristics might reflect the presence of an active fault in an area about morphotectonic analyses for identifying a Quaternary Fault. In this researched area, there are two watersheds namely Way Jambul and Way Belu watersheds. They come from Mount Rendingan flowing from the north (the upstream area) to the south (the downstream area) continuously into the sea through the Semangko Gulf. They have different morphotectonic characteristics due to the rocks and geological structures that develop in the area.

Ratio of Valley Floor Width to Valley Height (V_f)

Uplift levels in the researched area were observed through valley forms related to erosion type, not uplift level (U or V), where a high V_f value was associated with a low uplift velocity, so the river passes the riverbed towards the lateral direction. Uplift level of a region can be observed through the role of rivers that have the shape of the valley tends to be tenuous (U) and valleys that tend to be steep (V). The ratio of width and height value (V_f) is the value between the valley and the height or as the value of the comparison between the width and height of the valley, and is shown as the V_f calculation. High V_f values associate with low lifting rates, so the river cuts widely the valley floor laterally and the valley shape is widened. While low V_f values reflect the association with high uplift, so the valley will be more tapered (V) and erosion tends to be vertical. Based on the V_f values, in the researched area various uplift rates took place from low to high. According to Keller and Pinter (2002), Bull (2007), and Pérez-Peña *et al.* (2010), the Lower V_f values ($V_f < 1$) showed the V-shaped valleys and

usually connected with linear active down cutting streams. While higher V_f values ($V_f > 1$) are associated with U-shaped valleys as the response to relative low tectonic activity. For an example, here is shown one of V_f calculation result in the researched area such as in Way Jambul 7A sub-watersheds that have V_f value of 0.29 related to high uplift rate (Figure 4).

The calculation result of V_f at Way Jambu sub-watershed on the location numbers 1A, 5A, 6A, 7A, 9A, 10A, 11A, 12A, 14A, 15A, 17A, and 18A shows high uplift rates with V_f values in range from 0.18 to 0.45. While the location number of 3A, 8A, 13A, and 16A have moderate uplift rates with the value of V_f in range from 0.53 to 0.74.

Based on the result calculation of V_f at Way Belu watershed, the location number 1B, 9B, 10B, 14B, 15B, and 16B have the V_f values of 0.22 to 0.45 that tend to show high uplift rates. While the location of Way Belu watershed number 2B, 3B, 6B, 7B, 8B, 11B, and 13B a moderate uplift rate have occurred, shown by the V_f value in range from 0.54 to 0.94. Furthermore, location of Way Belu watershed number 4B, 5B, 12B, 17B, 18B,

19B, and 20B low uplift rate was shown by the V_f value in range from 1.49 to 6.57.

Moreover, locations of Way Jambul and Way Belu subwatersheds number of 2A, 4A, 18B, 19A, and 19B have a low uplift rate with V_f value ranging from 1.86 to 3.70, except two locations (18B and 20A) that have V_f value 6.75 to 7.50. They are obtained on the downstream part of Way Jambul watershed, in the southern part of the researched area.

Based on the result of all V_f calculation (Way Jambul and Way Belu watersheds), uplift rates scatter across the north to the southern part of the researched area, but the areas which have high uplift rate are located in the middle of the researched area. Furthermore, the result expressed low to high uplift rate with the value ranging from 0.75 - 0.60 as shown in Table 2 and Figure 5.

Mountain Front Sinuosity (S_{mf})

The calculation of mountain front sinuosity (S_{mf}) was done by determined the S_{mf} through observing the topography and position of the mountain front of Way Jambul and Way Beluwa-

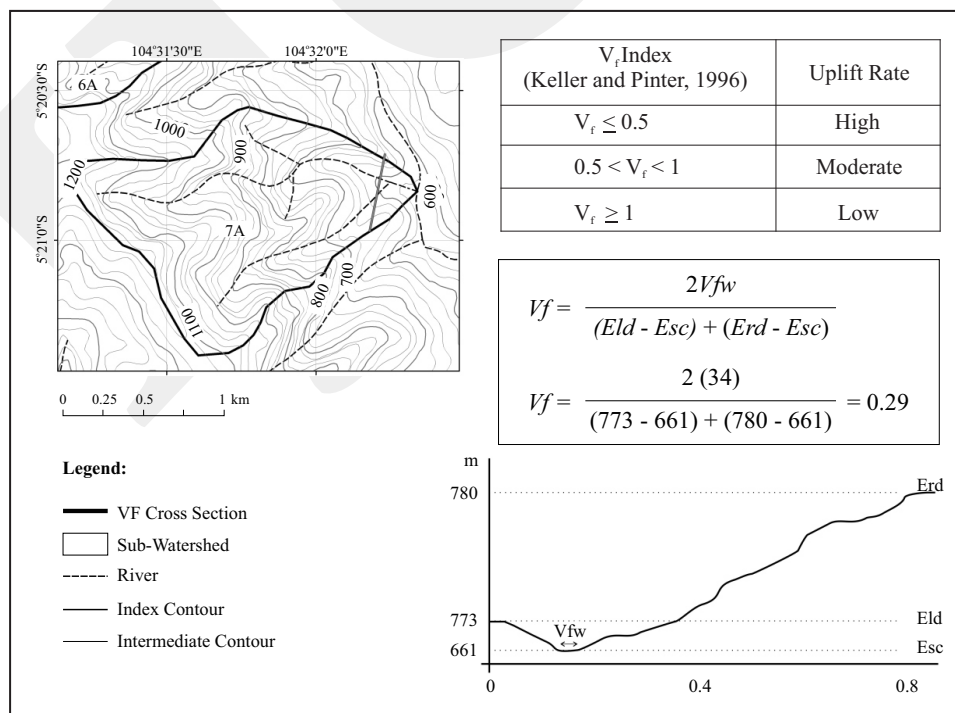


Figure 4. Illustration of Valley floor width to valley height ratio calculation (V_f). Here from V_f calculation result shows low V_f value is 0.29 and indicate the area has a high uplift rate.

Table 2. Valley Floor width to Valley Height Calculation (V_f) shows Low-moderate-high Uplift Rates in Way Jambul and Way Belu Watersheds. Determination of Uplift Rates follow Keller & Printer classifications (1996); $V_f \leq 0.5$ high, $0.5 < V_f < 1$ moderate, $V_f \geq 1$ low uplift rates.

Watershed	NSW ^(d)	vfw	2vfw	eld	erd	esc	V_f	Uplift Rate
Way Jambul	1A	60	120	1173	835	785	0.27	H ^(a)
Way Jambul	2A	93	186	926	876	851	1.86	L ^(c)
Way Jambul	3A	55	110	1127	1101	1023	0.60	M ^(b)
Way Jambul	4A	77	154	754	779	729	2.05	L ^(c)
Way Jambul	5A	35	70	1006	990	887	0.32	H ^(a)
Way Jambul	6A	74	148	1017	882	779	0.43	H ^(a)
Way Jambul	7A	34	68	780	773	661	0.29	H ^(a)
Way Jambul	8A	46	92	826	751	702	0.53	L ^(c)
Way Jambul	9A	24	48	792	890	788	0.45	H ^(a)
Way Jambul	10A	10	20	853	856	800	0.18	H ^(a)
Way Jambul	11A	12	24	868	883	837	0.31	H ^(a)
Way Jambul	12A	49	98	425	349	266	0.40	H ^(a)
Way Jambul	13A	83	166	591	681	524	0.74	M ^(b)
Way Jambul	14A	43	86	429	405	315	0.42	H ^(a)
Way Jambul	15A	66	132	730	779	599	0.42	H ^(a)
Way Jambul	16A	53	106	255	255	183	0.74	M ^(b)
Way Jambul	17A	57	114	430	354	266	0.45	H ^(a)
Way Jambul	18A	22	44	424	429	341	0.26	H ^(a)
Way Jambul	19A	20	40	75	50	55	2.67	L ^(c)
Way Jambul	20A	15	30	25	25	23	7.50	L ^(c)
Way Belu	1B	33	66	1191	1397	1141	0.22	H ^(a)
Way Belu	2B	13	26	982	948	941	0.54	M ^(b)
Way Belu	3B	27	54	794	788	755	0.75	M ^(b)
Way Belu	4B	32	64	755	782	747	1.49	L ^(b)
Way Belu	5B	58	116	694	691	675	3.31	L ^(b)
Way Belu	6B	82	164	743	829	675	0.74	M ^(b)
Way Belu	7B	98	196	759	749	637	0.84	M ^(b)
Way Belu	8B	33	66	782	802	750	0.79	M ^(b)
Way Belu	9B	36	72	811	912	763	0.37	H ^(a)
Way Belu	10B	22	44	1067	1144	968	0.16	H ^(a)
Way Belu	11B	23	46	760	761	726	0.67	M ^(b)
Way Belu	12B	33	66	712	692	685	1.94	L ^(c)
Way Belu	13B	25	50	728	711	693	0.94	M ^(b)
Way Belu	14B	33	66	438	467	341	0.30	H ^(a)
Way Belu	15B	36.6	73.2	400	366	302	0.45	H ^(a)
Way Belu	16B	10	20	313	307	275	0.29	H ^(a)
Way Belu	17B	43	86	230	210	206	3.07	L ^(c)
Way Belu	18B	69	138	55	62	48	6.57	L ^(c)
Way Belu	19B	122	244	134	77	62	2.80	L ^(c)
Way Belu	20B	29	58	79	54	45	1.35	L ^(c)

^(a)H=High, ^(b)M=Moderate, ^(c)L=Low, ^(d)NSW = Number of sub-watershed

tersheds to know the level of tectonic activity on the researched area. S_{mf} is an index reflecting the balance between force that has a tendency to cut along the mountain front and the tectonic force that directly produces a mountain face coinciding with the active fault zone which reflects the active tectonics. The S_{mf} calculation tends to indicate that the researched area is dominated by the active faults in the middle to the northern part of Way Belu. For

an example here is one of the S_{mf} calculations performed on the segment C that a value of mountain front sinuosity is 1.5 (Figure 6). Furthermore, all the result of S_{mf} calculation expressed that the area has moderate to active tectonic activities level with the value ranges between 2.09 to 1.05 (Figure 7).

The overall S_{mf} calculation results of fourteen segments produce S_{mf} values ranging from 1.05 to 2.09. Most of them are situated in an active

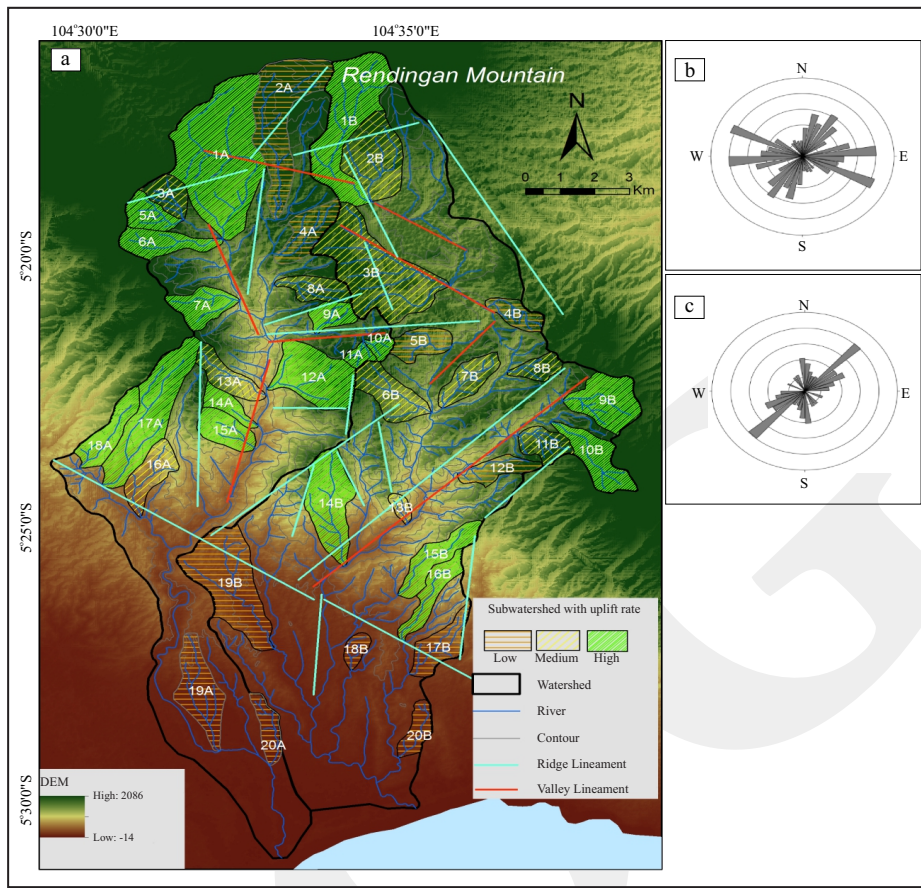


Figure 5. (a) Way Jambul and Way Belu Watersheds in the research area demonstrate the morphotectonic characteristics represented by NW - SE, NNE - SSW, NNW - SSE, and W - E structural directions showing the uplift rates from low to high, (b) Plotting rosette diagrams show the NW - SE lineament of ridges (N 294° - 336°) trending structures along the northern and western parts, (c) NE-SW valley lineaments (N 24° - 57°) trending structure along the southeast-eastern part of this area.

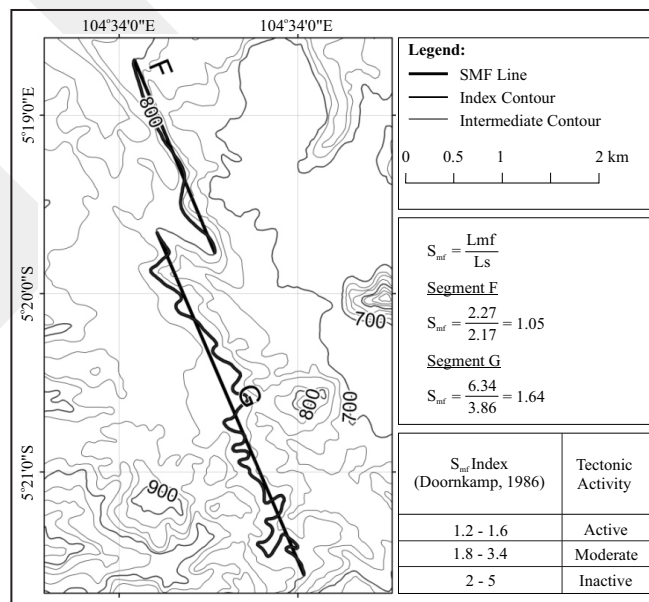


Figure 6. Illustration of two mountain front sinuosity calculation (S_{mf}) on the F and G segments of Way Belu watershed. Here is shown segment F having an smf value in an active tectonic position (1.05) as well as segment G that has an smf value 1.64 which are expressed into an active tectonic level (Doornkamp, 1986).

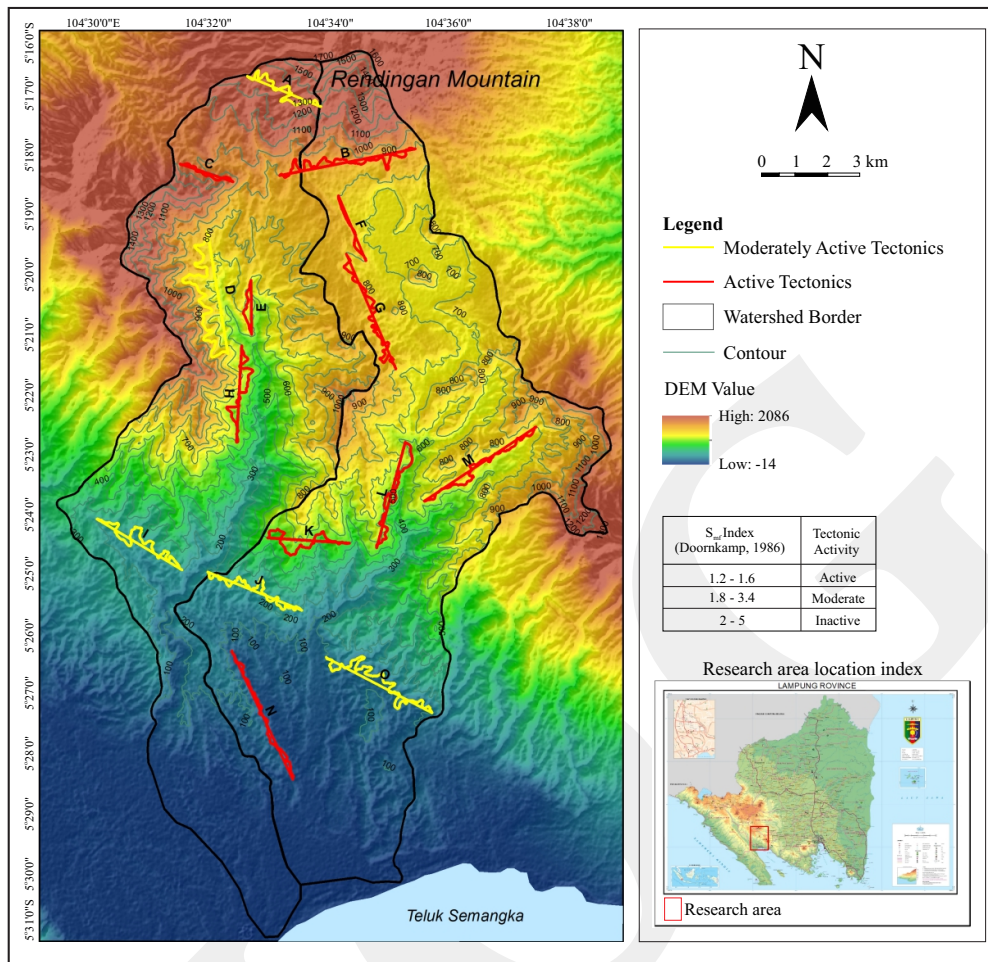


Figure 7. S_{mf} calculation map shows that from all the result of S_{mf} calculations expressed in the area have a high to low tectonic activity level with the value from 1.05 to 2.09 in ranges.

tectonic activity level. This characteristic can be described from S_{mf} values of active tectonic level such as: B (1.57), C (1.15), E (1.09), F(1.05), G(1.64), H(1.49), J(1.77), K(1.67), L(1.45), M(1.27), and N(1.13), except at five locations such as : A, D, I, J, and O that have S_{mf} values of moderate tectonic activity level such as: A (1.84), D (2.06), I (1.81), J (1.77), and O (2.09). According to S_{mf} index (Doornkamp, 1986) this area is controlled by active tectonics (Table 3).

Lineaments density analysis (L_d) is performed to sharpen the determination of zones that have high dominant lineament intensity describing rock permeability at depth. The calculation results of L_d will produce contour maps based on the absolute value of lineament density in an area. There are found geothermal manifestations that come to the surface from the reservoir through the rock

fracture due to the geological structures activity. It can be used as evidence that active tectonic activity passes the area. The result calculation shows that the highest values of L_d of this area which is represented by the orange to red color. The areas that have high L_d values indicate that those areas have high fracture intensities (L_d : 3 km^{-1}) forming weak zones or secondary porosity in igneous rocks to be permeable from igneous rock properties that were originally impermeable (Figure 8).

DISCUSSION

This chapter explains the relationship between the result of remote sensing analysis and field observation, to present valid data related to the tectonic activity which is found in the researched

Table 3. Various Tectonic Activity Levels from Moderate to Active Tectonic Level. In general, this area indicates the existence of active tectonics that represented by fourteen segments of mountain front. It represents a NW-SE fault direction. The moderate tectonic level represents trending NNE -SSW fault direction.

Segments of Mountain Front	L_{mf} (km)	L_s (km)	S_{mf} (L_{mf}/L_s)	Tectonic Activity Level
A	4.46	2.42	1.84	Moderate
B	6.67	4.25	1.57	Active
C	1.97	1.71	1.15	Active
D	7.92	3.85	2.06	Moderate
E	1.81	1.66	1.09	Active
F	2.27	2.17	1.05	Active
G	6.34	3.86	1.64	Active
H	4.43	2.98	1.49	Active
I	5.51	3.05	1.81	Moderate
J	5.49	3.11	1.77	Moderate
K	4.21	2.52	1.67	Active
L	4.89	3.38	1.45	Active
M	5.25	4.13	1.27	Active
N	4.95	4.38	1.13	Active
O	7.64	3.66	2.09	Moderate

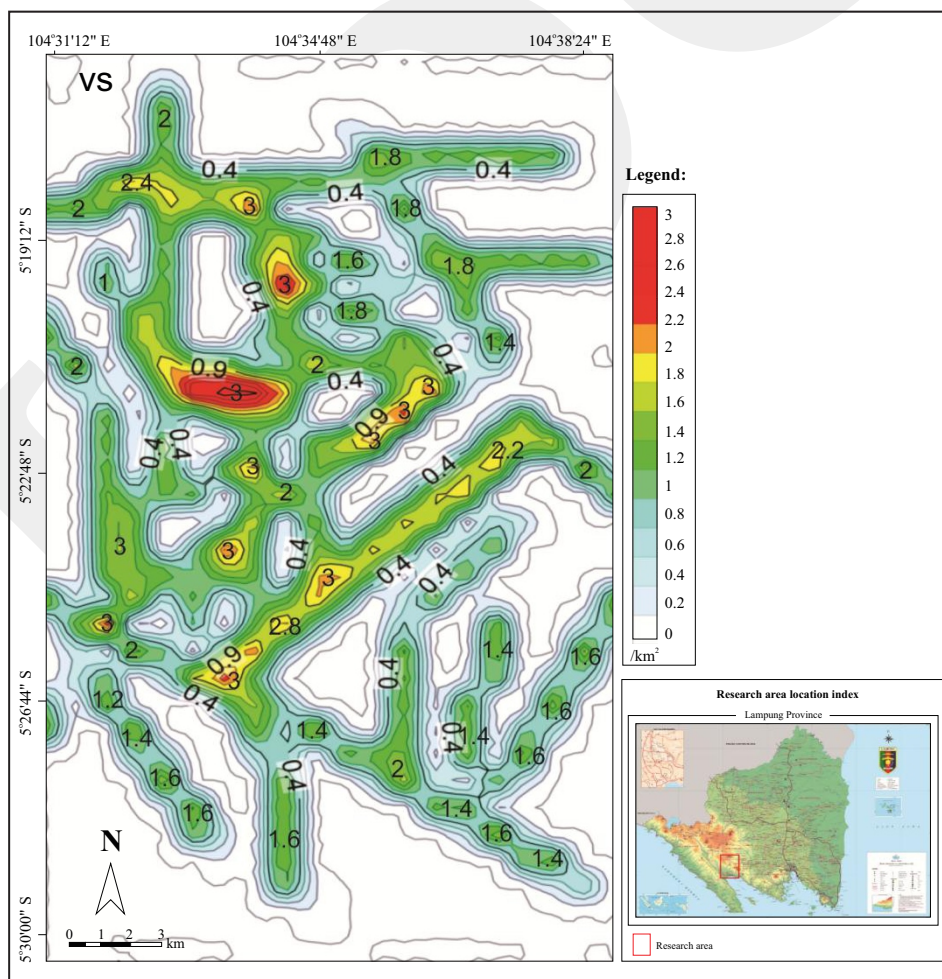


Figure 8. Map of lineament density (L_d) shows areas that have low to high density, forming a pattern that is relatively similar to the pattern of fault lines. Areas that have a high density have a range of L_d values from 2-3 km^2 (permeable rocks) which are colored orange to red.

area. Besides, it also explains physical properties, appearances, and distribution of geothermal surface manifestations that related to the role of the existing faults.

Analysis of lineaments density in the research area shows the values of lineament density (L_d) from low to high. Low lineament density is shown by L_d value less than 1 km^{-1} , and for areas that have a moderate lineament values spread on the inside of depression area with the values of L_d : $1 - 2 \text{ km}^{-1}$. Furthermore, the areas that have high lineament density values shown with orange to red colors with the values of L_d : $2 - 3 \text{ km}^{-1}$. The area that has a high L_d value has a pattern that is relatively similar to the fault pattern which passes liquid to the surface from subsurface hydrothermal systems.

Field Interpretation

Based on field observations in connection with remote sensing analysis results, the geological structure developed in the researched area shows a depression landform (caldera) which is surrounded by steep hills and valleys. In some places, it is indicated by fault scarps with the NE to SW, NW to SE, and W to the E directions which occur as normal and strike-slip faults. The existence of these fractures cut through the rock forming a secondary permeability. In addition, besides ridge and valley lineaments, elongated hills are also recognized as other geological structure indications such as triangular facet which has a steep slope.

The distribution of geothermal surface manifestations such as altered rocks, hot springs, mud pools, steaming ground, solfatara, and fumaroles is found at the intersection of ridge and valley with NW - SE, SW - NE, and W - E fault directions. The NW - SE fault present as a semi-circular depression graben is recognized to control the distribution of geothermal surface manifestations. In the researched area, the presence of two watersheds *i.e.* Way Jambul and Way Belucan be explained as follows:

Way Jambul Watershed

Way Jambul watershed occurs as long hills with NW to SE direction that becomes the up-

stream boundary as part of eastern Way Jambul watershed. Cotton (1948, in Doornkamp, 1986) stated that escarpment was one of units or morphological formations that closely related to tectonic, causing the fault areas tend to be susceptible to erosion and rock movement. Guidi *et al.* (2012) also stated that high escarpment (called "Timpe") of fault was a geomorphological evidence of an active fault. From the field observation, this area is cut through by tectonic activities. It can be identified by the presence of steep lineament of ridge and valleys, fault scarp, triangular facet, and rockslide found at some points of observation.

Way Belu Watershed

Way Belu watershed is present as long hills with NW to SE direction which becomes the upstream boundary as part of western Way Belu watershed. In the field, the lineaments are represented by hills, fault scarp, and rockslide. In some places, they are clearly visible. This confirms that the area is passed by the geological structure due to tectonic activities. The river flows at Way Belu watershed having a parallel pattern to the hills and valleys, indicate that the development of geological structures in the Mount Rendingan has NE to SW and W to E directions. Such geological structures are caused by the cutting in the rock forming a fracture zone that is appointed by rockslides in some places (Figure 9).

Geothermal Surface Manifestations

Geothermal surface manifestations are found as hot spring, mud pool, altered rock, steaming ground, steam heated water, solfatara, and fumaroles. The distribution of geothermal surface manifestations to the surface is due to geothermal heat fluid from the reservoir flows to the surface through permeable rocks with commonly vertical flow direction from reservoirs. According to Cumming (2009), the permeability distribution of a geothermal reservoir connects with its temperature. Commonly, the high temperature creates more permeability distribution flow.

The geothermal manifestations which are found at the first observation location in the up-

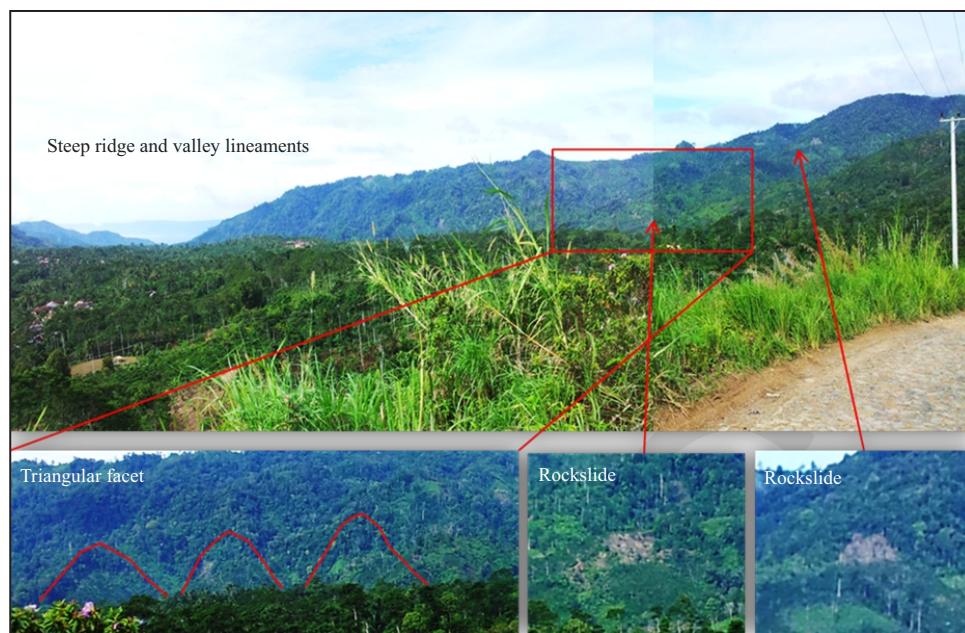


Figure 9. Morphotectonic phenomena in the research areas such as ridge and valley lineaments, triangular facets, and landslides found to reflect the area being controlled by an active tectonic activity. This phenomenon is evidenced by the occurrence of ridge and valley that extends to have NW-SE direction in the west and middle part of the researched area.

stream Way Belu watershed are fumarole, altered rock (kaolinite), steaming ground with temperature of 97.4°C, sulphur smelling, hot spring, turbid, water temperature of 94.8°C, pH of 3, and air temperature of 23°C. In the northern part of this area, there are three river branches with colourless, odourless, warm water temperature of 36°C, with pH of 3. The river flow rate is 0.04 m³/sec and the air temperature is 23°C.

The other geothermal surface manifestation at the second observation location is found in an expanse of altered basaltic andesitic lava. Such rock altered argillically within an acid condition is shown by the presence of kaolinite mineral. Megascopically, the existence of accessory minerals of pyrite, abundant chlorite, and quartz is determined. Altered rocks found in pyroclastic tuff breccia indicate as argillic prophyritic with accessory minerals such as kaolinite and chlorite. Hot spring temperature found at 97.2°C and a lot of bubble gases are found at the floor of the river. Within geothermal surface manifestation at the third observation location, steam heated water lake is found surrounded mostly by a quite dense vegetation, and it is characterized by steep hills. The physical properties of this water are

colourless, sulphur smelling, and pH of 4. The temperature of steam heated water (filling a lake) is 41.3°C due to heavy rain during the observation, while the air temperature is 28°C. It is estimated that the water is already mixed with surface water.

In another geothermal surface observation, at the fourth location in the downstream of Way Belu watershed at southern part of the researched area, highly fractured rock wall and slickenside which have fault strike of N 175°E / 88° and pitch 8°, and shows the presence of hot water gushing out periodically. The physical properties of hot spring are colourless, odourless with temperature of 99.4° C, and pH of 6. The water temperature at Way Belu floor river is 30° C which is similar to the air temperature, colourless, odourless, and has flow rate of 0.3 m³/sec. Geothermal surface manifestation at the fourth observation location is characterized by splashing colourless and odourless hot water, with the temperature of 91° C. The hot springs from rock fractures on the banks of streams have sharp turn flow directions. Massive lava and volcanic breccia step in as outcrop in this location.

The presence of colourless steamed heated water forming a lake with temperature of 94.6°C and pH of 4, with air temperature of 26°C, is a

geothermal surface manifestation observed in the fifth location. In this location, altered rock containing kaolinite is found quite extensive with smelled sulfuric fumarole and solfatara.

The field observation to the distribution of geothermal surface manifestations as explained above correlates to the morphotectonic calculations results in the Way Jambul and Way Belu watersheds. This strongly indicates that the researched area is characterized by the presence of an active tectonic activity level. It is reflected by the results of the V_f and S_{mf} calculations. V_f values of 0.18 up to 0.45 with S_{mf} values ranging between 1.05 - 1.64 indicate a high uplift rate landform. In addition, the presence of fractured fault and rock soil slopes which are resistant to the erosion, tends to indicate that the rockslide are associated with an active tectonic activity.

The surface geothermal manifestation found at the foot of Mount Rendingan comprises altered rock, steam heated water, steaming ground, and hot spring with temperature of 97.2° C. In this area gas bubbles are observed in the bottom of the river with the temperature of 91° - 94° C. The occurrence of these geothermal surface manifestations confirmed that the area is passed by fault forming fractures in the rock as a medium of geothermal manifestation to the surface. This is in line with the results of morphotectonic analysis that the area underwent high rates uplift condition confirming that the tectonic activity is continuous from the northern to the southern parts of the researched area with the direction of NW - SE. The development of geological structure that related to the distribution of the geothermal surface manifestations is shown clearly in Figures 10.

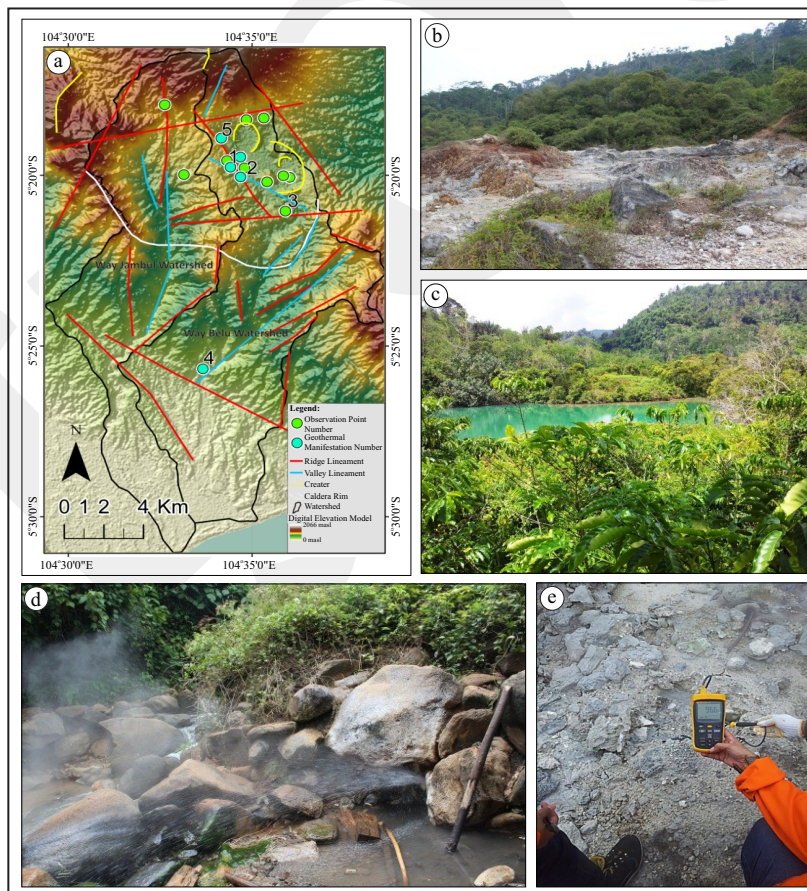


Figure 10. (a) Geological structure in the research area plays role to the appearances and distribution of the geothermal surface manifestations at the observation point number of 1,2,3,4 and 5; (b) Altered rock, steaming ground, fumarole, and solfatara. The steaming ground has temperature of 73° - 96° C in range, (c) Steam heated water has temperature of 61° C, (d) Hot water (splashing) has temperature of 91° C, (e) Steaming ground has temperature of 96.6° C. (Imagery source; Jarvis *et al.*, 2006).

CONCLUSIONS

From the topographic map, SRTM-DEM image, morphotectonic analysis, and field observation, it can be concluded that geological structures developing in the researched area have the trend directions of NE to SW, NW to SE, and W to E.

The result of morphotectonic analyses, such as V_f and S_{mr} calculations through analysis of ridges or hill and valley lineaments and segment of rivers quantitatively, has high uplift rates of tectonic activity which is supported by the values of valley floor width to valley height (V_f) ranging from 0.18 to 0.45, and mountain front sinuosity (S_{mr}) ranging from 1.05 to 2.09. The geothermal surface manifestations such as hot spring, steam heated water, steaming ground, altered rock, fumarole, and solfatara are found scatteredly on the area passed by faults that have NE to SW, NW to SE, and W to E directions. Moreover, the SW, NW to SE, and W to E faults control the distribution of the geothermal surface manifestations where the hot springs have the temperature ranging from 40° to 94° C and the steaming grounds have the temperature varying from 74° to 97° C. Therefore, these areas can be classified as potential geothermal sources according to morphotectonic indexes (V_f and S_{mr}) which affect the fractures in the rock, and those become paths for the appearance and distribution of geothermal surface manifestations.

ACKNOWLEDGEMENT

With great respect the author would like to thank the leader of Padjadjaran University who has provided internal grant funds in ALG. The author wish to acknowledge Mr.Siahaan from PT. Pertamina Geothermal Energy for his support. The author is also grateful to Dr. Nana Suwarna and Dr.Eng. Agus Didit Haryanto, M.Sc. for their patience and very useful guidance in writing the manuscript. Thanks are also due to Sofyan Isya Ansori, Murni Sulastri, and Pradnya Paramatha Raditya Rendra who have provided support and moral guidance.

REFERENCES

- Bhat, F.A., Bhat, I.M., Sana, H., Iqbal, M., and Mir, A.R., 2013. Identification of geomorphic signatures of active tectonics in the West Lidder watershed, Kashmir Himalayas using remote sensing and GIS. *International Journal of Geomatics and Geosciences*, 4 (1), p.164-176.
- Billings, M.P., 1972. *Structural Geology (3rd edition)*, Englewood Cliffs, Prentice-Hall, Inc., New Jersey, 591pp.
- Bull, B.W., 2007. *Tectonic Geomorphology of Mountains: A New Approach to Paleoseismology*, Blackwell Science Ltd., Australia, 305pp.
- Bull, B.W., and McFadden, L., 1977, Tectonic geomorphology North and South of the Garlock fault, California. *Proceedings of the 8th Annual Geomorphology Symposium*, Binghamton, New York, September, 23-24, p.115-138.
- Burbank, D.W., and Anderson R.S., 2001. *Tectonic Geomorphology*. Malden, Blackwell Science Ltd., Australia, 267pp.
- Cumming, W., 2009. Geothermal resource conceptual models using surface exploration data. *Proceedings of the 34th Workshop on geothermal reservoir engineering*, Stanford University, Stanford, California, February, 9-11, p.1-6.
- Doornkamp, J.C., 1986. Geomorphological approaches to the research of neotectonics. *International Journal of Geological Society*, 143, p.335-342.
- Ganas, A., Pavlides, S., Karastathis, 2005. DEM-based morphometry of range-front escarpments in Attica, central Greece, and its relation to fault slip rates. *Journal of Geomorphology*, 65 (3 - 4), p.301-319. DOI: 10.1016/j.geomorph.2004.09.006
- Gentana, D., Nurfadli, E., Syafri, I., Rosa, I.P.Y., and Sulastri, M., 2016. The role of physical-mechanical characteristic of weathered volcanic rock to the potential mass movement at the southern part of Garut, West Java Indonesia. *Proceeding of the 24th Annual Scientific Con-*

- ference and exhibitions. Federation International Surveyors, Christchurch, New Zealand, May, 2 - 6, p.1-12.*
- Gentana, D., Sulaksana, N., Sukiyah, E., and Yuningsih, E.T., 2017. Determination of Tanggamus geothermal prospect area, Lampung Provinces, Sumatra based on remote sensing and 3D micromine software. *Proceeding of the 25th Annual scientific conference & exhibitions. Federation International Surveyors, Helsinki, Finland, May, 29 - June, 2, p.1-13.*
- Goudie, S.A., 2004. *Encyclopedia of Geomorphology*. Routledge Ltd., New York, 1 (A-1), 1156pp.
- Guidi, G., Scudero, S., and Gresta, S., 2012. New insights into the local crust structure of Mt. Etna volcano from seismological and morphotectonic data. *Volcanology and Geothermal Research Journal*, Elsevier, p.83-92. DOI: 10.1016/j.jvolgeores.2012.02.001
- Hancock, 1994. *Continental Deformation*. Pergamon press, New York, 421pp.
- Jarvis, A., Reuter, H.I., Nelson, A., Guevara, E., 2006. Hole-filled seamless SRTM data V3, 514 *International Centre for Tropical Agriculture (CIAT)*, available from 515. <http://srtm.csi.cgiar.org>.
- Jelinek, J., 2008. Morphotectonic analysis of digital relief model - A suitable means of searching for zones of rock mass brittle failure. *Geo-Science Engineering*, LIV (3), p. 1-13.
- Kamah, M.Y., 2001, Mapping permeability potential as target reservoir at geothermal Ulubelu field. *Proceeding of the 5th INAGA annual scientific conference and exhibitions, Yogyakarta, March, 7-10, p.1-5.* (in Indonesian).
- Keller, E.A. and Pinter, N., 1996. *Active Tectonics; earthquakes, uplift and landscape (2nd edition)*, Prentice-Hall, Inc., New Jersey, 359pp.
- Kirianov, V.Y., 2007. *Geography of volcanic zones and distribution of active volcanoes. Natural and Human Induced Hazards*, 1, p.1-21.
- Linsley, J.G., Kohler, A.M., and Paulhus, H.L.J., 1949. *Hydrology For Engineering*, Mc-Graw Hill Book Company Inc., United State of America, 358pp.
- McCaffrey, R., 2009. *The Tectonic Framework of The Sumatran Subduction Zone. Earth and Environmental Sciences*, Rensselaer Polytechnic Institute, Troy, New York, 365pp.
- Muljana, B., 2006, Tectonic extension of the Sunda Bay. *Bulletin of Scientific Contribution*, 4 (2), p.137-145 (in Indonesian with English abstract).
- O'Rourke, T.D., Jung, J.K., and Argyrou, C., 2016. Underground pipeline response to earthquake-induced ground deformation. *International Journal of Soil Dynamics and Earthquake Engineering*, Elsevier, p.272-283. DOI: 10.1016/j.soildyn.2016.09.008
- Pérez-Peña, J.V., Azor, A., Azañón, J.M., and Keller, E.A., 2010. Active tectonics in the Sierra Nevada: Insights from geomorphic indexes and drainage pattern analysis. *International Journal of Geomorphology*, Elsevier, p.74-87. DOI: 10.1016/j.geomorph.2010.02.020
- Ritter, D.F., Kochel, C.R., and Miller, J.R., 2002. *Process Geomorphology (4th edition)* Mc.Graw-Hill Company, New York, 560pp.
- Scheidegger, A.E., 2004. *Morphotectonics*. Springer, Heidelberg, Berlin, 197pp.
- Siahaan, E.E., 1998. Hydrothermal Eruption Mapping Report of Ulubelu. Geothermal Division, E & P Directorate, Lampung, Unpublished, 43pp. (in Indonesian).
- Sukiyah, E., Syafri, I., Sjafrudin, A., Nurfadli, E., Khaerani, P., and Simanjuntak, P.A.D., 2015. Morphotectonic and satellite imagery analysis for identifying quaternary faults at southern part of Cianjur-Garut region, West Java, Indonesia. *Proceeding of the 36th Asian Conference on Remote Sensing, Philippine, October, 19-23, p.1-10.*
- Sukiyah, E., Syafri, I., Winarto, B.J., Susilo, B., Saputra, A., and Nurfadli, E., 2016. Active faults and their implications for regional development at the southern part of West Java, Indonesia. *Proceeding of the 24th Annual scientific conference and exhibitions. Federation International Surveyors, Christchurch, New Zealand, May, 2 - 6, p.1-13.*

- Sukiyah, E., Pranantya, A.P., Dwinuryana, S., and Jones, M., 2017. The morphotectonic 3-D modeling of Cisadane watershed based on interpretation of satellite and field survey in the region of South Tangerang, West Java, Indonesia. *Proceeding of the 25th Annual scientific conference and exhibitions. Federation International Surveyors, Helsinki, Finland*, May, 29 - June, 2, p.1-13.
- Van Noordwijk, V.M., Agus, F., Suprayogo, D., Hairah, K., Pasya, G., Verbist, B., and Farida., 2004. The role of agroforestry in watershed hydrological functions (DAS), *Journal of Agricultural Sciences*, Brawijaya University, 26 (1), p.1-8. (in Indonesian with English abstract).
- Van Zuidam, R.A., 1983. Terrain Analyses And Classification Using Aerial Photograph, A Geomorphological Approach. *International Institute for Aerial Survey and Earth Sciences, Netherlands*, VII, 325pp.
- Wilson, P., Rais, J., Reigber, C., Reinhart, E., Ambrosius, B.A.C., Le Pichon, X., Kasser, M., Suharto, P., Majid, A., Othman, A.H., Almeda, R., and Boonphakdee, C., 1998. Study provides data on active plate tectonics in Southeast Asia region. *EOS Transactions. American Geophysical Union*, 79 (45), p.545-556. DOI: 10.1029/98EO00398
- Wilson, J.P., 2000. *Terrain Analysis: Principles and Applications*. John Wiley and Sons, Inc., New York, 479pp.
- Yudhicara, Muslim, D., Sudradjat, A., 2017. Geomorphic analysis in determining tectonic activity affected by Sumatra Fault in Liwaregion and its surrounding area, Lampung, Indonesia. *Indonesian Journal on Geosciences*, 4 (3), p.193-208. DOI: 10.17014/ ijog. 4.3.193-208.
- Zobin, V.M., 2017, *Introduction to Volcanic Seismology (3rd edition)*. Elsevier, 582pp.